Spectrochimica Acta Part A 76 (2010) 410–417

Contents lists available at ScienceDirect

Spectrochimica Acta Part A: Molecular and Biomolecular Spectroscopy

journal homepage: www.elsevier.com/locate/saa

Interaction of alpinetin with bovine serum albumin: Probing of the mechanism and binding site by spectroscopic methods

Guowen Zhang*, Nan Zhao, Xing Hu, Jiao Tian

State Key Laboratory of Food Science and Technology, Nanchang University, 235, Nanjing East Road, Nanchang 330047, Jiangxi, China

ARTICLE INFO

Article history:
Received 23 February 2010
Received in revised form 24 March 2010
Accepted 8 April 2010

Keywords:
Alpinetin
Bovine serum albumin
Fluorescence quenching
Binding site
Fourier transform infrared spectroscopy

ABSTRACT

The binding interaction between alpinetin and bovine serum albumin (BSA) in physiological buffer solution (pH 7.4) was investigated by fluorescence, UV–vis spectroscopy and Fourier transform infrared (FT-IR) spectroscopy. It was proved from fluorescence spectra that the fluorescence quenching of BSA by alpinetin was probably a result of the formation of BSA–alpinetin complexes, and the binding constant (K_a) were determined according to the modified Stern–Volmer equation. The thermodynamic parameters, enthalpy change (ΔH) and entropy change (ΔS), were calculated to be 22.10 kJ mol^{-1} and 166.04 J mol^{-1} K^{-1}, respectively, which indicated that the interaction between alpinetin and BSA was driven mainly by hydrophobic interaction. Moreover, the competitive experiments of site markers suggested that the binding site of alpinetin to BSA was located in the region of subdomain IIA (sudlow site I). The binding distance (r) between the donor (BSA) and the acceptor (alpinetin) was 3.32 nm based on the Förster theory of non-radioactive energy transfer. In addition, the results of synchronous fluorescence and FT-IR spectra demonstrated that the microenvironment and the secondary structure of BSA were changed in the presence of alpinetin.

1. Introduction

Protein–drug interactions have aroused great interest in recent years. Investigating the binding of drugs to proteins can provide useful information of the structural features that determine the therapeutic effectiveness of drugs. Thus, the studies on this aspect have been an important research field in life science, chemistry, and clinical medicine. Serum albumin, the most abundant protein in the blood circulatory system, plays an important role in the transport and deposition of a variety of endogenous and exogenous substances [1,2]. Bovine serum albumin (BSA), one of the major components in plasma protein, is frequently used in biophysical and biochemical studies since it has a well-known primary structure, and it has been associated with the binding of many different categories of small molecules, such as dye, drugs and toxic chemicals [3–5]. In this work, BSA was selected as our study protein model because of its low cost, ready availability, unusual ligand-binding properties, medical importance and particularly its structural homology with human serum albumin (HSA) [6,7].

Flavonoids are a large group of polyphenolic natural products that are widely distributed in plants of higher genera. Such compounds are found to possess novel therapeutic properties of high potency and low systemic toxicity [8]. In this context the question of possible target molecules and the mode of interactions with targets constitute an important focus of current pharmacological research on flavonoids. In recent years, the binding mechanism between flavonoids and proteins has attracted much attention. Many reports on this aspect are available in the literature [9–15]. In previous works, we studied the binding properties of serum albumins with some flavonoids including icariin and chrysin [16,17]. Alpinetin (7-hydroxy-5-methoxyflavanone, structure shown in Fig. 1), one of the abundant natural flavonoids, is the main active component of *Alpinia katsumadai* Hayata, which is one herbal medicine commonly used in China [18]. It has already been reported as an anti-tumor, anti-bacterial and anti-inflammatory agent [19].

Fluorescence spectroscopy is a powerful and simple method to study the interaction of small molecule with protein, because of its high sensitivity, reproducibility and convenience [20,21]. It can reveal the accessibility of quenchers to fluorophores, help to understand the binding mechanisms of small molecule to albumin. Circular dichroism (CD) spectroscopy and Fourier transform infrared (FT-IR) spectroscopy are widely used to detect the change in conformation of protein [22]. Pan et al. [23] investigated the interaction of gold nanorod with BSA at pH 7.4 by fluorescence spectroscopy. They found that gold nanorod–albumin solution has a strong fluorescence emission peaked at 351 nm after being excited with a wavelength of 280 nm, and the magnitude of fluorescence intensity increased with increasing nanorod concentration. The binding constant and the binding capacity of gold nanorod to BSA were determined, which indicated that the nanoparticle shape may

* Corresponding author. Tel.: +86 7918305234; fax: +86 7918304347.
E-mail address: gwzhang@ncu.edu.cn (G. Zhang).

1386-1425/$ – see front matter © 2010 Elsevier B.V. All rights reserved.
doi:10.1016/j.saa.2010.04.009

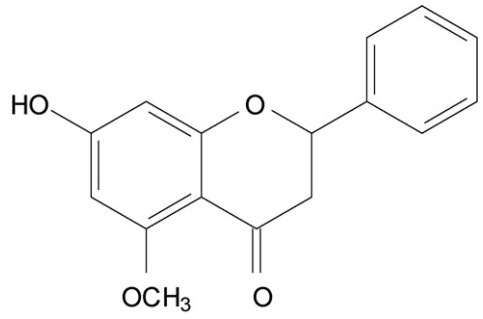

Fig. 1. Molecular structure of alpinetin.

have strong influence upon the link between gold nanorod and blood components. Cheng and Zhang [24] reported that quenching mechanism of fluorescence of BSA by salidroside was a static quenching by forming the BSA–salidroside complexes. The binding of salidroside to BSA was driven by the hydrogen bonds and van der Waals forces. There was one class of binding sites for salidroside towards BSA, and salidroside most likely binds to the hydrophobic pocket located in subdomain IIA. Furthermore, they detected the conformational changes of BSA in the presence of salidroside by CD spectroscopy and FT-IR spectroscopy.

In this paper, the interaction between alpinetin and BSA was studied under physiological pH conditions by fluorescence, UV–vis spectroscopy and FT-IR spectroscopy. Many attempts were made to explore the binding mechanism, the special binding site and the effect of alpinetin on the conformational changes of BSA. We hope that this work can benefit understanding the transportation and metabolic process of the drug at molecular level.

2. Experimental

2.1. Materials

Bovine serum albumin (BSA) was purchased from Sino-American Biotechnology (Beijing, China) and used without further purification. The BSA working solutions were prepared to be the concentration of 6.25×10^{-7} mol L^{-1} in Tris–HCl buffer solutions (0.10 mol L^{-1} Tris base, 0.10 mol L^{-1} HCl and 0.10 mol L^{-1} NaCl, pH 7.4). Alpinetin (analytical grade) was obtained from National Institute for the Control of Pharmaceutical Biological Products (Beijing, China). The stock solution (9.61×10^{-4} mol L^{-1}) of alpinetin was prepared in absolute ethanol. All other reagents and solvents were of analytical grade and doubly distilled water was used throughout the experiment. All stock solutions were stored at 0–4 °C.

2.2. Apparatus

All fluorescence spectra were measured on a Hitachi spectrofluorimeter Model F-4500 equipped with a 150 W Xenon lamp and a thermostat bath. The widths of both the excitation slit and emission slit were set at 5.0 nm. The absorption spectra were measured on a Shimadzu UV-2450 spectrophotometer. A quartz cell of 1.0 cm was used for the measurements. FT-IR spectra were measured on a Nicolet Nexus 670 FT-IR spectrometer (America) equipped with a Germanium attenuated total reflection (ATR) accessory, a DTGS KBr detector and a KBr beam splitter.

2.3. Procedure

2.3.1. Fluorescence measurements

A quantitative analysis of the potential interaction between alpinetin and BSA was performed by fluorimetric titration. A 3.0 ml solution, containing 6.25×10^{-7} mol L^{-1} BSA, was titrated by successive additions of alpinetin solution (to give a final concentration of 2.31×10^{-5} mol L^{-1}). Titrations were done manually by using micro-injector. The fluorescence emission spectra were measured at 298, 304 and 310 K in the wavelength range of 300–540 nm with exciting wavelength at 280 nm. The synchronous fluorescence spectra were obtained by simultaneously scanning the excitation and emission monochromators. It was recorded at $\Delta\lambda = 15$ and 60 nm in the absence and presence of various amounts of alpinetin over a wavelength range of 270–330 and 250–320 nm, respectively. The appropriate blanks corresponding to the buffer solution were subtracted to correct background of fluorescence.

2.3.2. Site marker competitive experiments

Binding location studies between alpinetin and BSA in the presence of three site markers (warfarin, ibuprofen and digitoxin) were measured using the fluorescence titration methods. The concentrations of BSA and warfarin/ibuprofen/digitoxin were all kept at 6.25×10^{-7} mol L^{-1}. Alpinetin was then gradually added to the BSA–warfarin/ibuprofen/digitoxin systems. Fluorescence spectra were recorded at 298 K with an excitation wavelength of 280 nm in the range of 300–540 nm.

2.3.3. UV–vis absorbance and FT-IR measurements

The UV–vis absorption spectra were obtained by scanning the solution on a Shimadzu UV-2450 spectrophotometer with the wavelength range of 300–500 nm. The operations were carried out at room temperature.

FT-IR measurements were carried out at room temperature on a Nicolet Nexus 670 FT-IR spectrometer (America). All spectra were taken via the ATR method with resolution of 4 cm^{-1} and 60 scans. Spectra processing procedures: spectra of buffer solution were collected at the same condition. Then, subtract the absorbance of buffer solution from the spectra of sample solution to get the FT-IR spectra of protein. The subtraction criterion was that the original spectra of protein solution between 2200 and 1800 cm^{-1} was featureless [25].

3. Results and discussion

3.1. Measurement of fluorescence spectra

For macromolecules, fluorescence measurements can give some information about the binding of small molecule substances to protein, such as the binding mechanism, binding constants, binding sites, and intermolecular distances. For BSA, there are only three intrinsic fluorophores-tryptophan, tyrosine and phenylalanine. Actually, the intrinsic fluorescence of BSA is almost contributed by tryptophan alone, because phenylalanine has a very low quantum yield and the fluorescence of tyrosine is almost totally quenched if it is ionized, or near an amino group, a carboxyl group, or a tryptophan. That is, the change of intrinsic fluorescence intensity of BSA is that of fluorescence intensity of tryptophan residue when small molecule substances are added to BSA [26].

Fluorescence spectra of BSA were determined in the presence of increasing amount of alpinetin, as shown in Fig. 2. It is obvious that BSA has a strong fluorescence emission peaked at 342 nm after being excited with a wavelength of 280 nm. When a fixed concentration of BSA was titrated with different amounts of alpinetin, a remarkable intrinsic fluorescence decrease and the obvious red shift at the maximum wavelength of BSA was observed. This suggested that the microenvironment around BSA was changed after the addition of alpinetin [27]. Furthermore, alpinetin caused an accompanying enhancement around the emission wavelength of 436 nm (Fig. 2, curve k, alpinetin only), suggesting that there was

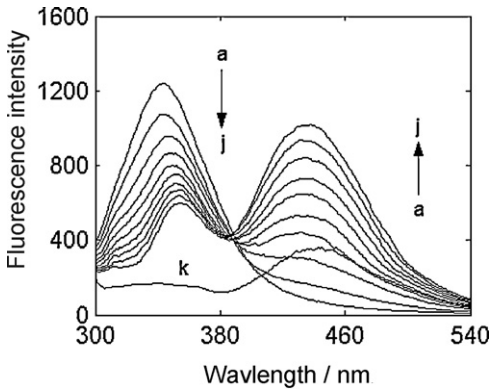

Fig. 2. Effect of alpinetin on fluorescence spectra of BSA (T = 298 K, pH 7.4, λ_{ex} = 280 nm). c(BSA) = 6.25 × 10^{-7} mol L^{-1}; c(alpinetin)/(×10^{-5} mol L^{-1}), a–j: 0, 0.26, 0.51, 0.77, 1.02, 1.28, 1.54, 1.79, 2.05, 2.31, respectively. Curve k shows the emission spectrum of alpinetin only, c(alpinetin) = 6.25 × 10^{-6} mol L^{-1}.

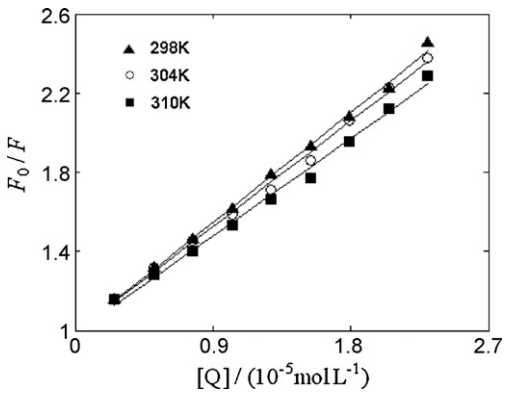

Fig. 3. The Stern–Volmer plots for the quenching of BSA by alpinetin at different temperatures (λ_{ex} = 280 nm, λ_{em} = 342 nm). c(BSA) = 6.25 × 10^{-7} mol L^{-1}.

a strong association and non-radioactive energy transfer between alpinetin and BSA. The occurrence of an isoactinic point at 388 nm might also indicate the existence of bound and free alpinetin in equilibrium [28].

3.2. Determination of quenching mechanism

Fluorescence quenching refers to any process which is a decrease of the fluorescence intensity from a fluorophore due to a variety of molecular interactions. These include excited-state reactions, molecular rearrangements, energy transfer, ground-state complex formation and collisional quenching. Quenching can occur by different mechanisms, which usually classified as dynamic quenching and static quenching. Dynamic and static quenching can be distinguished by their different dependence on temperature of binding constants and viscosity, or preferably by lifetime measurements. Generally, the quenching constants decrease with increasing temperature for static quenching, but the reverse effect is for dynamic quenching [29,30].

For the dynamic quenching, the mechanism can be described by the Stern–Volmer equation (Eq. (2)) [29]:

$$\frac{F_0}{F} = 1 + K_{SV}[Q] = 1 + K_q\tau_0[Q] \quad (1)$$

where F_0 and F are the fluorescence intensities of BSA in the absence and presence of the quencher, respectively. K_q is the quenching rate constant of the biomolecule, K_{SV} is the Stern–Volmer dynamic quenching constant, τ_0 is the average lifetime of the biomolecule without quencher. The value of τ_0 of the biopolymer is 10^{-8} s^{-1} [31], and [Q] is the concentration of quencher.

Eq. (1) was applied to determine K_{SV} by linear regression of a plot of F_0/F against [Q], and $K_{SV} = K_q\tau_0$. The results are shown in Fig. 3. The values of K_{SV} and K_q at different temperatures (298, 304 and 310 K) are shown in Table 1. The results showed that the values of Stern–Volmer quenching constants K_{SV} decreased with increasing temperature, which indicated that the probable quenching mechanism of BSA–alpinetin interaction was initiated by complex formation rather than by dynamic collision. Generally, the maximum scatter collision quenching constant, K_q of various kinds of quenchers with biopolymer is 2 × 10^{10} L mol^{-1} s^{-1} [31]. However, the rate constants for the quenching of BSA caused by alpinetin are greater than the K_q for the scatter mechanism. This confirms that the fluorescence quenching is not the result of dynamic collision quenching, rather a consequence of static quenching [29,32].

Table 1
Stern–Volmer quenching constants for the interaction of alpinetin with BSA at different temperatures.

pH	T (K)	K_{SV} (×10^4 L mol^{-1})	K_q (×10^{12} L mol^{-1} s^{-1})	R^a
7.4	298	6.159	6.159	0.9990
	304	5.913	5.913	0.9981
	310	5.453	5.453	0.9970

[a] R is the correlation coefficient.

Therefore, the quenching data were expressed via the modified Stern–Volmer equation [33]:

$$\frac{F_0}{\Delta F} = \frac{1}{f_a K_a}\frac{1}{[Q]} + \frac{1}{f_a} \quad (2)$$

where ΔF is the difference of fluorescence in the absence and presence of the quencher at concentration [Q], f_a is the fraction of accessible fluorescence, K_a is the effective quenching constant for the accessible fluorophores.

The dependence of $F_0/\Delta F$ on the reciprocal value of the quencher concentration 1/[Q] is the linear with slope equal to the value of $1/f_aK_a$. The value of $1/f_a$ is fixed on the ordinate. The constant K_a is the quotient of an ordinate $1/f_a$ and slope $1/f_aK_a$. The corresponding values of K_a at three different temperatures are summarized in Table 2. The values of K_a increased with the rising temperature, which indicated that the binding is endothermic reaction [34], and the capacity of alpinetin binding to BSA is enhanced with the increasing temperature.

3.3. Thermodynamic analysis and the nature of the binding forces

The interaction forces between small molecules and biomolecules mainly include hydrogen bonds, van der Waals force, hydrophobic force, and electrostatic interactions. The signs and magnitudes of thermodynamic parameters for protein reactions can be account for the main forces contributing to protein stability. If the enthalpy change (ΔH) does not vary significantly over the temperature range studied, then its value and that of entropy change (ΔS) can be determined from the van't Hoff equation:

$$\log K_a = -\frac{\Delta H}{2.303RT} + \frac{\Delta S}{2.303R} \quad (3)$$

In Eq. (3), R is gas constant. The temperatures used were 298, 304 and 310 K. The values of ΔH and ΔS were obtained from the slope and intercept of the linear van't Hoff plot based on log K_a versus $1/T$. The free energy change (ΔG) was then evaluated from the following equation:

$$\Delta G = \Delta H - T\ \Delta S \quad (4)$$

Table 2 lists the thermodynamic parameters for the interaction of alpinetin with BSA. The values of ΔH and ΔS were 22.10 kJ mol^{-1} and 166.04 J mol^{-1} K^{-1}, respectively, which indicated that the

Table 2
Modified Stern–Volmer association constants K_a and relative thermodynamic parameters of the BSA–alpinetin system.

T (K)	K_a ($\times 10^4$ L mol^{-1})	R^a	ΔH (kJ mol^{-1})	ΔG (kJ mol^{-1})	ΔS (J mol^{-1} K^{-1})	R^b
298	6.338	0.9999	22.10	−27.38	166.04	0.9975
304	7.416	0.9988		−28.38		
310	8.957	0.9950		−29.38		

[a] R is the correlation coefficient for the K_a values.
[b] R is the correlation coefficient for the van't Hoff plot.

formation of BSA–alpinetin was mainly an endothermic and entropy-driven reaction. The negative value of ΔG reveals that the interaction process is spontaneous. The positive ΔH and ΔS values indicate that hydrophobic force plays a major role in the binding of alpinetin to BSA [35].

3.4. Identification of the binding sites of alpinetin on BSA

For the static quenching interaction, if it is assumed that there are independent binding sites to a set of equivalent sites on a macromolecule. The apparent binding constant and the number of binding sites can be determined according to the following equation [36]:

$$\log\frac{F_0 - F}{F} = \log\ K_b + n\log[\mathrm{Q}] \quad (5)$$

where K_b and n are the apparent binding constant and the number of binding sites for BSA–alpinetin system, respectively. Thus, the intercept and slope value of the plot, $\log(F_0–F)/F$ versus log[Q] give the K_b and n values. From Eq. (5), the values of K_b and n at 298 K were obtained to be 6.180×10^4 L mol^{-1} and 1.001, respectively. The high linear correlation coefficient R (0.9997) indicated that assumptions underlying the derivation of Eq. (5) were convincible. The value of n approximately equal to 1 suggested that there was one class of binding sites for alpinetin towards BSA.

There are two distinct drug-binding sites, sites I and II in serum albumin, which are located within specialized cavities in subdomains IIA and IIIA, respectively [37,38]. They present the similar chemical properties, bringing some difficulties to some extent for completely characterizing the specific binding sites of ligands to BSA. Sudlow et al. [39] have suggested that site I of serum albumin showed affinity for warfarin, phenylbutazone, etc., and site II for ibuprofen, flufenamic acid, etc. The binding of digitoxin was found to be independent of sites I and II [40,41]. In order to identify the alpinetin binding site on BSA, competition experiments were performed with warfarin, ibuprofen and digitoxin as per Sudlow's classification of the binding sites.

The fluorescence spectra of BSA–warfarin/ibuprofen/digitoxin system with various concentrations of alpinetin are shown in Fig. 4 at 298 K with excitation wavelength of 280 nm. As shown in Fig. 4A, with the addition of warfarin to the BSA solution, the fluorescence intensity was significantly lower than that of without warfarin, and the maximum emission wavelength of BSA had an obvious red shift. In contrast, there was no obvious variety with the addition of ibuprofen or digitoxin (shown in Fig. 4B and C). Then, alpinetin was added to the solutions of BSA and site markers in equimolar concentrations. It can be seen that the fluorescence intensity change of BSA with the increasing concentration of alpinetin in the absence (Fig. 2) and presence (Fig. 4B and C) of ibuprofen/digitoxin were almost the same. On the contrary, the fluorescence intensity in the case of warfarin (Fig. 4A) differed but decreased dramatically at the same condition, which indicated that alpinetin was significantly displaced by warfarin. In addition, the fluorescence peak of the alpinetin at approximately 436 nm in the presence of ibuprofen/digitoxin was higher than that of the system in the presence of warfarin, implying the formation of a new fluorescence substance.

In order to compare the effect of probes on BSA–alpinetin system more directly, the experiment data were analyzed by the modified Stern–Volmer equation (shown in Fig. 5), and the binding constants of BSA–alpinetin system in the presence of different site markers

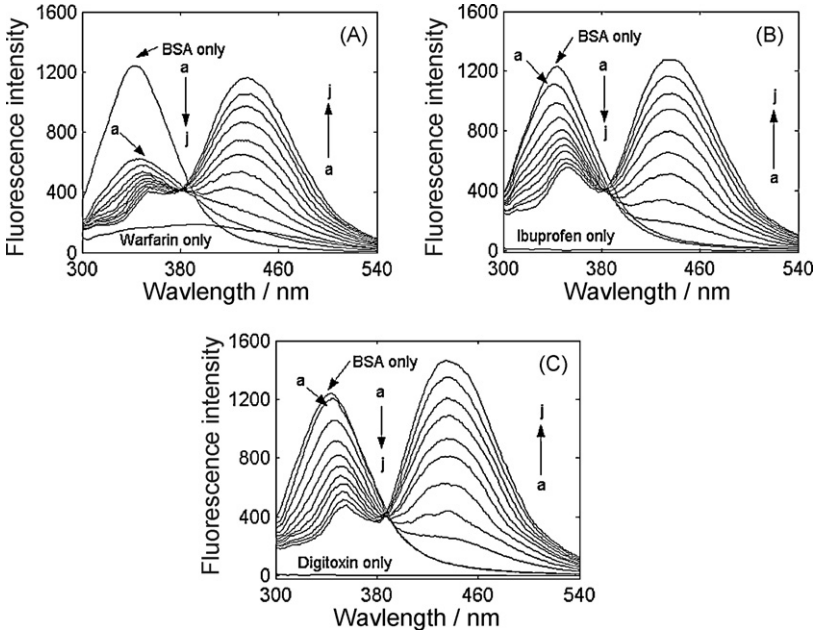

Fig. 4. Effect of site markers to BSA–alpinetin system (T = 298 K, λ_{ex} = 280 nm). (A) c(BSA) = c(warfarin) = 6.25×10^{-7} mol L^{-1}; (B) c(BSA) = c(ibuprofen) = 6.25×10^{-7} mol L^{-1}; (C) c(BSA) = c(digitoxin) = 6.25×10^{-7} mol L^{-1}; c(alpinetin)/($\times 10^{-5}$ mol L^{-1}), a–j: 0, 0.26, 0.51, 0.77, 1.02, 1.28, 1.54, 1.79, 2.05, 2.31, respectively.

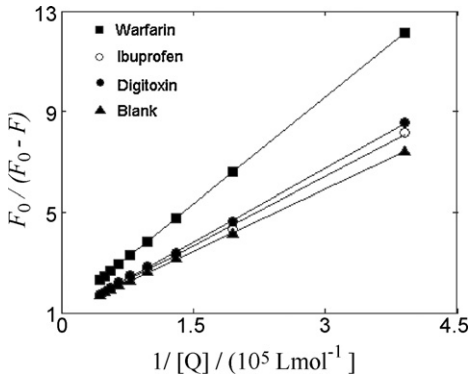

Fig. 5. The results of site markers competitive experiments of BSA–alpinetin system.

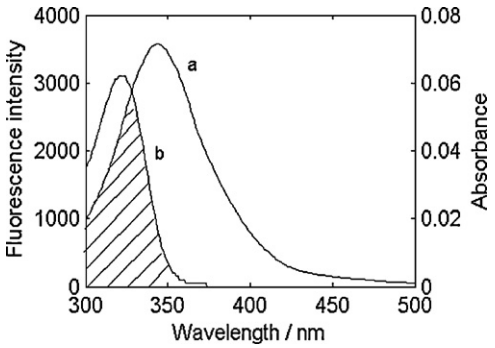

Fig. 6. Spectral overlaps of the fluorescence spectra of BSA (a) with the absorption spectra of alpinetin (b). c(BSA) = c(alpinetin) = 2.0×10^{-6} mol L^{-1}.

were calculated (Table 3). Obviously, warfarin could significantly influence the binding of alpinetin to BSA, whereas ibuprofen or digitoxin had a lesser effect on the binding of alpinetin to BSA. Above evidences revealed that the binding site of alpinetin to BSA mainly located within subdomain IIA (site I).

3.5. Energy transfer between alpinetin and BSA

The binding distance (r) between a protein residue (donor) and a bound drug molecule (acceptor) can be calculated from the Föster's theory [42]. The efficiency of energy transfer (E) is related to the distance (R_0) between donor and acceptor by:

$$E = 1 - \frac{F}{F_0} = \frac{R_0^6}{R_0^6 + r^6} \quad (6)$$

where r is the distance between donor (BSA) and acceptor (alpinetin) and R_0 is the critical distance when their transfer efficiency is 50%. It is given by the following equation:

$$R_0^6 = 8.79 \times 10^{-25} K^2 n^{-4} \phi J \quad (7)$$

where K^2 is the spatial orientation factor of the dipole, N is the refractive index of medium, ϕ is the quantum yield of the donor, and J is the overlap integral of the fluorescence emission spectrum of the donor with the absorption spectrum of the acceptor (shown in Fig. 6), which can be calculated by the equation:

$$J = \frac{\int_0^\infty F(\lambda)\varepsilon(\lambda)\lambda^4 d\lambda}{\int_0^\infty F(\lambda) d\lambda} \quad (8)$$

where $F(\lambda)$ is the fluorescence intensity of the fluorescence donor at wavelength λ, and $\varepsilon(\lambda)$ is the molar absorption coefficient of the acceptor at wavelength λ. In the present case, $K^2 = 2/3$, $N = 1.336$, and $\phi = 0.118$ [43]. Thus, According to Eqs. (6)–(8), we were able to calculate the following parameters, $J = 1.19 \times 10^{-14}$ cm^3 L mol^{-1}, $R_0 = 2.53$ nm, $E = 0.160$, and $r = 3.32$ nm. The donor to acceptor distance is less than 8 nm, and $0.5R_0 < r < 1.5R_0$, which indicates the energy transfer from BSA to alpinetin occurred with great possibility [44]. In accordance with prediction by Förster's non-radiative energy transfer theory, these results again indicate the presence of static quenching mechanism in the interaction between alpinetin and BSA.

Table 3
Binding constants of competitive experiments of BSA–alpinetin system.

Site marker	K_a ($\times 10^4$ L mol^{-1})	R^a	SD[b]
Blank	6.338	0.9999	0.012
Digitoxin	5.060	0.9994	0.024
Ibuprofen	4.655	0.9997	0.017
Warfarin	3.806	0.9998	0.020

[a] R is the correlation coefficient.
[b] SD is the standard deviation.

3.6. Conformational investigations

The synchronous fluorescence spectra present the information about the molecular microenvironment in the vicinity of the fluorophore. The shift in position of maximum emission wavelength in the synchronous fluorescence spectra corresponds to the changes of polarity around the fluorophore. When the D-value ($\Delta\lambda$) between excitation wavelength and emission wavelength were set at 15 or 60 nm, the synchronous fluorescence can provide the characteristic information of tyrosine residues or tryptophan residues in BSA [45], respectively. By investigating the synchronous fluorescence spectra of tyrosine residues or tryptophan residues, we could explore the conformational changes of BSA. The synchronous fluorescence spectra of BSA upon addition of alpinetin at $\Delta\lambda = 15$ and 60 nm are shown in Fig. 7. It can be seen that a slight red shift (from 283.6 to 286.8 nm in Fig. 7B) of maximum emission wavelength of tryptophan residues was observed, whereas the fluorescence band of tyrosine residues blue shifts slightly from 289.2 to 286.4 nm (Fig. 7A). The former indicated that the conformation of BSA was somewhat changed, leading to the polarity around tryptophan residues strengthened and the hydrophobicity weakened [46]. The latter suggested that the polarity around tyrosine residues was decreased and the hydrophobicity increased [45,47].

In order to gain more information in physicochemical properties of alpinetin, the FT-IR spectroscopic measurements were performed on BSA and the BSA–alpinetin complexes. It can be reflected in the FT-IR spectra if the protein secondary structure changed in the BSA–alpinetin complexes. Infrared spectra of proteins exhibit a number of amide bands, which represent different vibrations of the peptide moiety. Among these amide bands of the protein, the protein amide I in the region 1600–1700 cm^{-1} (mainly C=O stretch) and amide II band in the region 1500–1600 cm^{-1} (C–N stretch couple with N–H bending mode) both have a relation ship with the secondary structure of protein, and the amide II band absorbance intensity has been reported to be proportional to the amount of protein absorbed, and is believed not to be very sensitive to the conformation of the protein [48,49]. Fig. 8 shows the FT-IR spectra of free BSA in Tris–HCl buffer and the difference spectra after binding with alpinetin. From Fig. 8, it can be seen that the peak position of the amide I band move from 1652 to 1645 cm^{-1} and amide II band shift from 1545 to 1513 cm^{-1} in BSA infrared spectra after addition of alpinetin. The second derivative of the FT-IR spectra for free BSA and the spectra for BSA binding with alpinetin are shown in Fig. 9. The peak positions of amide I bands in BSA infrared spectra shifted: 1614–1618, 1640–1644, 1666–1678 and 1687–1695 cm^{-1} after interaction with alpinetin. The changes of these peak positions and peak shapes demonstrated

Table 4
Secondary structure analysis for amide I region in free BSA and its alpinetin complexes at pH 7.4.

Systems	α-Helix (%)	β-Antiparallel (%)	β-Sheet (%)	β-Turn (%)	Random coil (%)
Free BSA	49	4	7	14	26
BSA–alpinetin	31	6	12	13	38

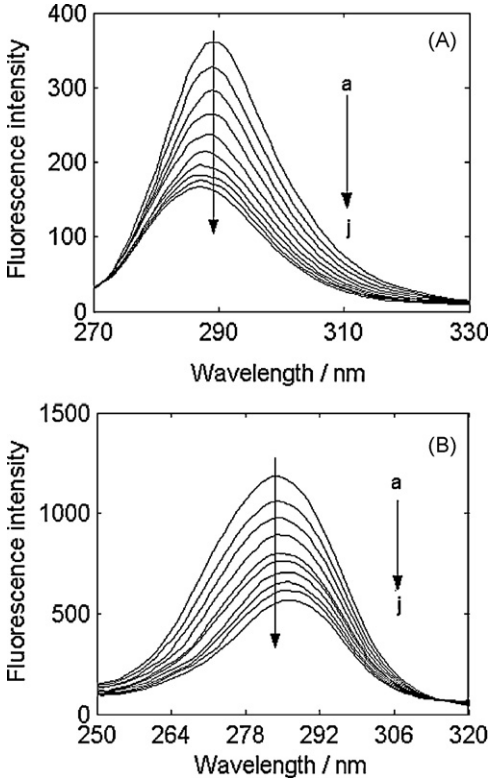

Fig. 7. The synchronous fluorescence spectra of BSA in the presence of alpinetin (T = 298 K, pH 7.4). c(BSA) = 6.25 × 10^{-7} mol L^{-1}; c(alpinetin)/(×10^{-5} mol L^{-1}), a–j: 0, 0.26, 0.51, 0.77, 1.02, 1.28, 1.54, 1.79, 2.05, 2.31, respectively. (A) Δλ = 15 nm and (B) Δλ = 60 nm.

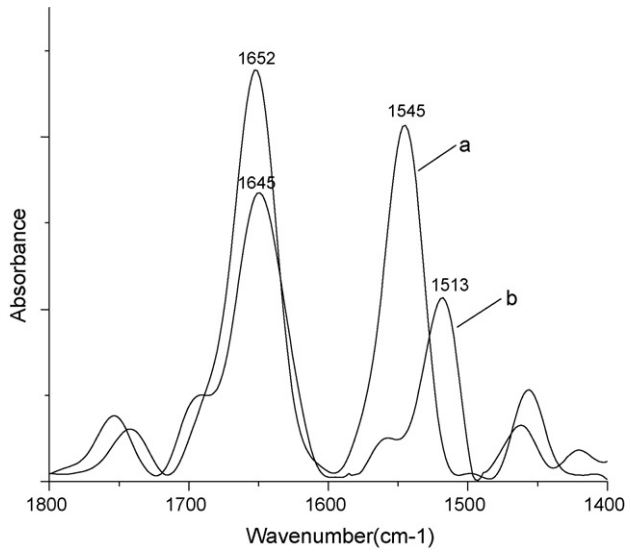

Fig. 8. FT-IR spectra of free BSA (a) and difference spectra [(BSA–alpinetin)–alpinetin] (b) in buffer solution in the region of 1800–1400 cm^{-1}, c(BSA) = 5.13 × 10^{-5} mol L^{-1}, c(alpinetin) = 9.61 × 10^{-5} mol L^{-1}, pH 7.4.

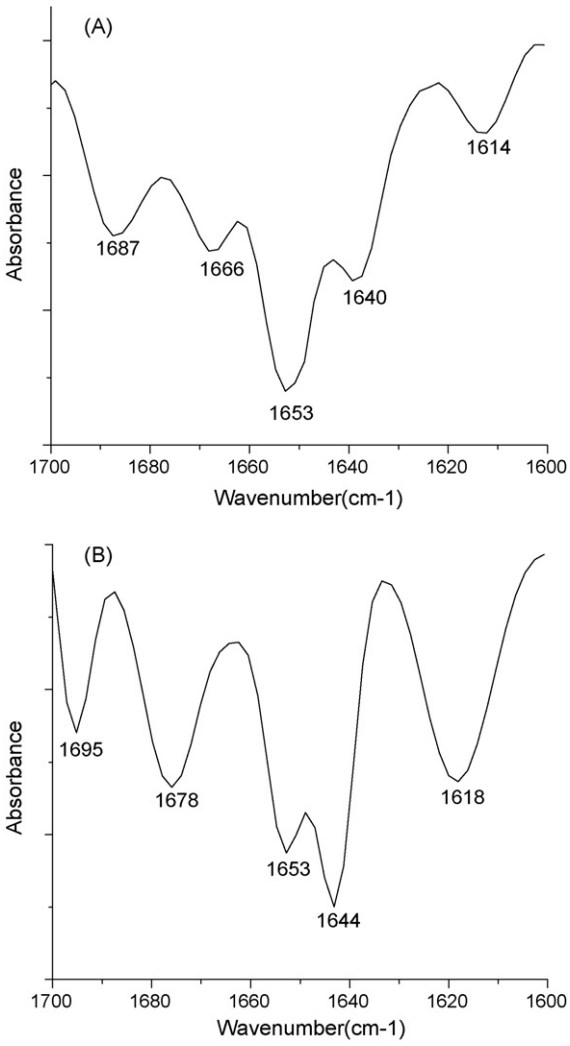

Fig. 9. Second-derivative resolution enhancement of free BSA (A) and its alpinetin complexes (B).

that the secondary structure of BSA has been changed because of the interaction of alpinetin with BSA.

Fig. 10 shows a quantitative analysis of the protein secondary structure of BSA before and after the interaction with alpinetin in Tris–HCl buffer. Based on the literature [50,51] in which the component bands of amides I were attributed according to the well-established assignment criterion, the data obtained from Fig. 10 are summarized in Table 4. It was found that the free BSA contained major amounts of α-helix 49% (1652 cm^{-1}), β-sheet 7% (1616 cm^{-1}), β-turn structure 14% (1666 cm^{-1}), β-antiparallel 4% (1687 cm^{-1}) and random coil 26% (1640 cm^{-1}). Upon alpinetin interaction, a major decrease of α-helix from 49% to 31% and minor decrease of β-turn from 14% to 13% with increases in random coil from 26% to 38%, β-sheet from 7% to 12% and β-antiparallel 4–6%. The decrease in α-helix structure and increase in random coin and β-sheet suggested a partial protein unfolding in the presence of alpinetin [52].

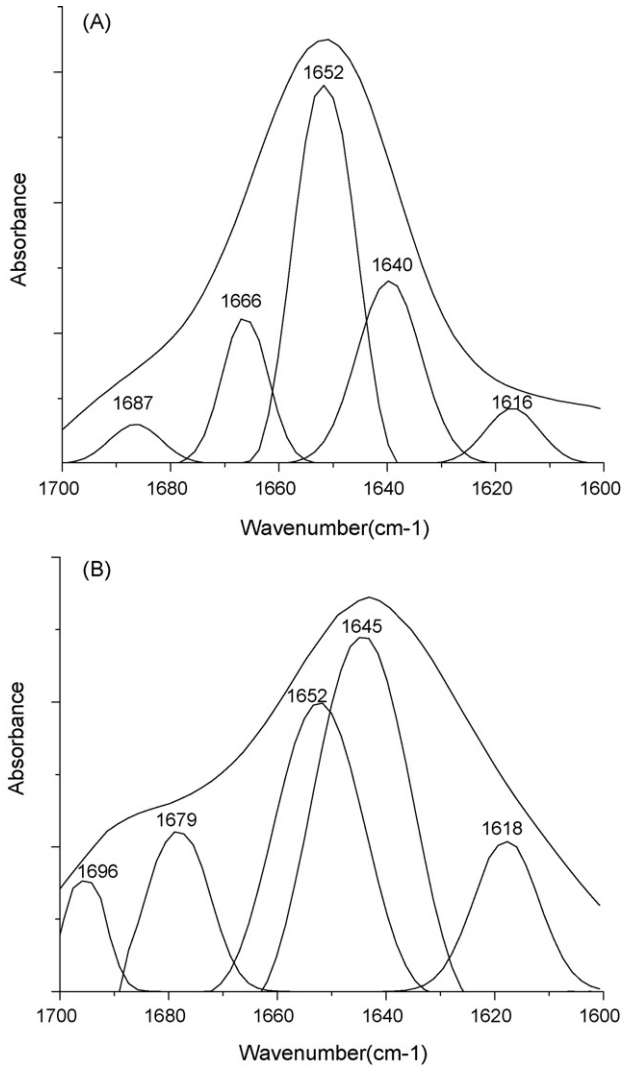

Fig. 10. Curve-fitted amide I region (1700–1600 cm^{-1}) of free BSA (A) and its alpinetin complexes (B).

4. Conclusions

Fluorescence, UV–vis absorption and FT-IR spectroscopic methods were applied to investigate the interaction between BSA and alpinetin in physiological buffer solution (pH 7.4). The quenching mechanism of fluorescence of BSA by alpinetin was a static quenching by forming the BSA–alpinetin complexes. The positive values of thermodynamic parameters (ΔH and ΔS) suggested that alpinetin could bind to BSA mainly through hydrophobic force. Site marker competitive experiments indicated that the binding of alpinetin to BSA primarily took place in subdomain IIA. The binding distance r was 3.32 nm based on Förster theory, which indicated that there was a non-radioactive energy transfer between BSA and alpinetin. Experimental results obtained from synchronous fluorescence and FT-IR spectra demonstrated that the binding of alpinetin to BSA induced some microenvironmental and conformational change of BSA.

Acknowledgements

The authors gratefully acknowledge the financial support of this study by the Jiangxi Province Natural Science Foundation (2009GZH0069, 2007GZH1924), the Research Program of State Key Laboratory of Food Science and Technology of Nanchang University (SKLF-TS-200917, SKLF-MB-200807), the Program of Science and Technology of Jiangxi Province (2009BNA09000) and the Foundation of Analytical and Test of Nanchang University (No. 2008006).

References

[1] D.C. Carter, J.X. Ho, Adv. Protein Chem. 45 (1994) 153–203.
[2] K. Yamasaki, T. Maruyama, U. Kragh-Hansen, M. Otagiri, Biochem. Biophys. Acta 1295 (1996) 147–157.
[3] P.N. Naik, S.A. Chimatadar, S.T. Nandibewoor, Spectrochim. Acta Part A 73 (2009) 841–845.
[4] X.L. Shi, X.W. Li, M.Y. Gui, H.Y. Zhou, R.J. Yang, H.Q. Zhang, Y.R. Jin, J. Lumin. 130 (2010) 637–644.
[5] G.C. Zhang, Y.Q. Wang, H.M. Zhang, S.H. Tang, W.H. Tao, Pestic. Biochem. Physiol. 87 (2007) 23–29.
[6] S. Ashoka, J. Seetharamappa, P.B. Kandagal, S.M.T. Shaikh, J. Lumin. 121 (2006) 179–186.
[7] X.L. Han, P. Mei, Y. Liu, Q. Xiao, F.L. Jiang, R. Li, Spectrochim. Acta Part A 74 (2009) 781–787.
[8] J.B. Harborne, H. Baxter, The Handbook of Natural Flavonoids, vol. 1, Wiley, New York, 1999, pp. 645–687.
[9] D.J. Li, J.F. Zhu, J. Jin, J. Photochem. Photobiol. A: Chem. 189 (2007) 114–120.
[10] A. Banerjee, K. Basu, P.K. Sengupta, J. Photochem. Photobiol. B: Biol. 90 (2008) 33–40.
[11] J.H. Li, C.L. Ren, Y.H. Zhang, X.Y. Liu, X.J. Yao, Z.D. Hu, J. Mol. Struct. 885 (2008) 64–69.
[12] J.S. Mandeville, E. Froehlich, H.A. Tajmir-Riahi, J Pharm. Biomed. Anal. 49 (2009) 468–474.
[13] T.H. Wang, Z.M. Zhao, L. Zhang, L. Ji, J. Mol. Struct. 937 (2009) 65–69.
[14] Y.M. Yang, Q.L. Hu, Y.L. Fan, H.S. Shen, Spectrochim. Acta Part A 69 (2008) 432–436.
[15] I. Matei, M. Hillebrand, J. Pharm. Biomed. Anal. 51 (2010) 768–773.
[16] G.W. Zhang, Q.M. Que, J.H. Pan, J.B. Guo, J. Mol. Struct. 881 (2008) 132–138.
[17] G.W. Zhang, X.X. Chen, J.B. Guo, J.J. Wang, J. Mol. Struct. 921 (2009) 346–351.
[18] Editorial committee of the pharmacopoeia of People's Republic of China, Pharmacopoeia of People's Republic of China (part one), Chemical Industry Press, Beijing, 1999.
[19] V. Cody, E. Middleton, J.B. Harborne, Plant Flavonoids in Biology and Medicine: Biochemical, Pharmacological and Structure Activity Relationships, Alan R. Liss, New York, 1986.
[20] A. Kathiravan, M. Chandramohan, R. Renganathan, S. Sekar, J. Mol. Struct. 919 (2009) 210–214.
[21] S.Y. Bi, Y.T. Sun, C.Y. Qiao, H.Q. Zhang, C.M. Liu, J. Lumin. 129 (2009) 541–547.
[22] X.F.L.X. Zhang, Y. Liu, J.F. Xiang, L. Li, Y.L. Tang, J. Mol. Struct. 888 (2008) 145–151.
[23] B.F. Pan, D.X. Cui, P. Xu, Q. Li, T. Huang, R. He, F. Gao, Colloid Surf. A: Physicochem. Eng. Aspects 295 (2007) 217–222.
[24] Z.G. Cheng, Y.T. Zhang, J. Mol. Struct. 889 (2008) 20–27.
[25] A.C. Dong, P. Huang, W.S. Caughey, Biochemistry 29 (1990) 3303–3306.
[26] H. Gao, L.D. Lei, J.Q. Liu, Q. Kong, X.Q. Chen, Z.D. Hu, J. Photochem. Photobiol. A: Chem. 167 (2004) 213–221.
[27] T. Yuan, A.M. Weljie, H.J. Vogel, Biochemistry 37 (1998) 3187–3195.
[28] Y.Z. Zhang, J. Dai, X. Xiang, W.W. Li, Y. Liu, Mol. Biol. Rep. 37 (2010) 1541–1549.
[29] J.R. Lakowicz, Principles of Fluorescence Spectroscopy, second ed., Plenum Press, New York, 1999, pp. 237–265.
[30] J. Chen, X.Y. Jiang, X.Q. Chen, Y. Chen, J. Mol. Struct. 876 (2008) 121–126.
[31] J.R. Lakowicz, G. Weber, Biochemistry 12 (1973) 4161–4170.
[32] G.Z. Chen, X.Z. Huang, J.G. Xu, Z.Z. Zheng, Z.B. Wang, The Methods of Fluorescence Analysis, second ed., Beijing Science Press, 1990.
[33] S.S. Lehrer, Biochemistry 10 (1971) 3254–3263.
[34] Y.Q. Wang, H.M. Zhang, G.C. Zhang, W.H. Tao, S.H. Tang, J. Mol. Struct. 830 (2007) 40–45.
[35] D.P. Ross, S. Subramanian, Biochemistry 20 (1981) 3096–3102.
[36] Y.J. Hu, Y. Liu, J.B. Wang, X.H. Xiao, S.S. Qu, J. Pharm. Biomed. Anal. 36 (2004) 915–919.
[37] G. Sudlow, D.J. Birkett, D.N. Wade, Mol. Pharmacol. 11 (1975) 824–832.
[38] D.C. Carter, X.M. He, Science 249 (1990) 302–303.
[39] G. Sudlow, D.J. Birkett, D.N. Wade, Mol. Pharmacol. 12 (1976) 1052–1061.
[40] T. Peters, All About Albumin: Biochemistry, Genetics and Medical Applications, Academic, San Diego, CA, 1995.
[41] A. Gerbanowski, C. Malabat, C. Rabiller, J. Gueguen, J. Agric. Food Chem. 47 (1999) 5218–5226.
[42] T. Förster, O. Sinanoglu (Eds.), Modern Quantum Chemistry, vol. 3, Academic Press, New York, 1996, p. 93.
[43] S. Kasai, T. Horie, T. Mizuma, S. Awazu, J. Pharm. Sci. 76 (1987) 387–392.

[44] S.F. Sun, B. Zhou, H.N. Hou, Y. Liu, G.Y. Xiang, Int. J. Biol. Macromol. 39 (2006) 197–200.
[45] W.C. Albert, W.M. Gregory, G.S. Allan, Anal. Biochem. 213 (1993) 407–413.
[46] B. Klajnert, M. Bryszewska, Bioelectrochemistry 55 (2002) 33–35.
[47] Y.Q. Wang, H.M. Zhang, G.C. Zhang, W.H. Tao, Z.H. Fei, Z.T. Liu, J. Pharm. Biomed. Anal. 43 (2007) 1869–1875.
[48] K. Rahmelow, W. Hubner, Anal. Biochem. 241 (1996) 5–11.
[49] Y.Y. Yue, Y.H. Zhang, Y. Li, J.H. Zhu, J. Qin, X.G. Chen, J. Lumin. 128 (2008) 513–520.
[50] M. Jiang, M.X. Xie, D. Zheng, Y. Liu, X.Y. Li, X. Chen, J. Mol. Struct. 692 (2004) 71–80.
[51] X.H. Liu, P.X. Xi, F.J. Chen, Z.H. Xu, Z.Z. Zeng, J. Photochem. Photobiol. B 92 (2008) 98–102.
[52] J.S. Mandeville, E. Froehlich, H.A. Tajmir-Riahi, J. Pharm. Biomed. Anal. 49 (2009) 468–474.